Similarities between the Hubbard and Periodic Anderson Models at Finite Temperatures

K. Held,[1] C. Huscroft,[2] R. T. Scalettar,[3] and A. K. McMahan[4]
[1]*Theoretische Physik III, Universität Augsburg, 86135 Augsburg, Germany*
[2]*Physics Department, University of Cincinnati, Cincinnati, Ohio 45221-0011*
[3]*Physics Department, University of California, Davis, California 95616*
[4]*Lawrence Livermore National Laboratory, University of California, Livermore, California 94550*
(Received 3 May 1999)

The single band Hubbard and the two band periodic Anderson Hamiltonians have traditionally been applied to rather different physical problems—the Mott transition and itinerant magnetism, and Kondo singlet formation and scattering off localized magnetic states, respectively. In this paper, we compare the magnetic and charge correlations, and spectral functions, of the two systems. We show quantitatively that they exhibit remarkably similar behavior, including a nearly identical topology of the finite temperature phase diagrams at half filling. We address potential implications of this for theories of the rare earth "volume collapse" transition.

PACS numbers: 71.27.+a, 71.10.Fd, 71.30.+h

The single band Hubbard model (HM) and the two band periodic Anderson model (PAM) have a long history in the study of many body effects in solids. While they have been proposed to describe complex d- and f-electron systems, respectively, the detailed atomic physics and orbital structure are nevertheless eliminated, leaving minimal Hamiltonians where the interplay between electron kinetic energy, screened electron-electron repulsion, the Pauli principle, temperature, and electron density still give rise to a rich variety of phenomena.

The key features of the half-filled HM are antiferromagnetism and a Mott insulator-metal transition within the paramagnetic phase [1,2]. Originally [3], the Mott transition was associated with a change in the density of states (DOS) from widely separated upper and lower Hubbard bands to a broad one-peak structure, and an accompanying loss of local moments. The key features of the PAM are magnetism arising from an indirect Ruderman-Kittel-Kasuya-Yosida interaction of the local moments mediated by the conduction electrons, and a DOS which, in the paramagnetic phase, has a three-peak structure—upper and lower bands and an additional Abrikosov-Suhl resonance near the Fermi surface [4]. Concomitant with the development of this resonance, local moments become screened by the conduction electrons, and an anomalous sharp feature in the free energy is observed [5]. During the past years, it has been established by dynamical mean-field theory (DMFT) [2,6] and quantum Monte Carlo (QMC) simulations [7] that the HM also has a three-peak structure in its paramagnetic DOS, thereby blurring at least one of the features believed to distinguish the two models.

It is the purpose of this paper to note even greater similarity between the two models at finite temperature, especially if a more physical choice is taken for the interband hybridization in the PAM. Specifically, our new DMFT results show that the f electrons of the PAM undergo a transition similar to the Mott transition of the HM, as is reflected by the f-electron spectral function, quasiparticle weight, and charge compressibility. Furthermore, the phase diagrams, at finite temperature, associated with the two models are topologically equivalent.

These similarities are of particular interest in that the HM [8] and PAM (or its impurity approximation [9]) have been proposed as competing models for the "volume-collapse" transitions in the rare earth and actinide metals. These pressure-induced phase transitions are characterized by unusually large (9%–15%) volume changes, and are believed to arise from f-electron correlation effects [10,11]. The present paper suggests that the predictions of the two models are more similar than has previously been thought, and that perceived incompatibilities may have arisen in part from differing and less rigorous approximations used in the treatment of electron correlations, as, for example, in mean-field-like local-density functional theory [11].

The single band HM is given by

$$H = \sum_{k\sigma} \epsilon_k^f f_{k\sigma}^\dagger f_{k\sigma} + U_f \sum_i \left(n_{if\uparrow} - \frac{1}{2}\right)\left(n_{if\downarrow} - \frac{1}{2}\right). \tag{1}$$

Here $\epsilon_k^f = \epsilon_0^f - 2t_{ff}[\cos(k_x) + \cos(k_y) + \cos(k_z)]$ is the nearest-neighbor band dispersion, where the energy scale is set by $t_{ff} = 1$, and U_f is the f-electron local interaction on every lattice site i. The two band PAM is

$$H = \sum_{k\sigma} [\epsilon_k^d d_{k\sigma}^\dagger d_{k\sigma} + \epsilon_k^f f_{k\sigma}^\dagger f_{k\sigma} + V_k(d_{k\sigma}^\dagger f_{k\sigma} + \text{H.c.})] + U_f \sum_i \left(n_{if\uparrow} - \frac{1}{2}\right)\left(n_{if\downarrow} - \frac{1}{2}\right), \tag{2}$$

where V_k denotes the hybridization between f and d electrons at momentum k. In the PAM, the d electrons are chosen to have the same nearest-neighbor dispersion as the f electrons of the HM ($t_{dd} = 1$), while the f electrons are chosen to be dispersionless, $t_{ff} = 0$. We study the "symmetric" PAM, i.e., $\epsilon_0^{d(f)} = 0$ and chemical potential $\mu = 0$, which has the property that $\langle n_f \rangle = \langle n_d \rangle = 1$ for

all choices of U_f, $t_{dd(ff)}$, hybridization strengths, and temperature T. Finally, we choose a nearest-neighbor intersite hybridization $V_k = -2t_{fd}[\cos(k_x) + \cos(k_y) + \cos(k_z)]$, but also have investigated the more canonical on-site hybridization $V_k = \sqrt{3}\,t_{fd}$, as well as an odd-parity nearest-neighbor form $V_k = -it_{fd}[\sin(k_x) + \sin(k_y) + \sin(k_z)]$. The three choices have zero, constant, and maximal $|V_k|$ on the half-filled Fermi surface, respectively, and yield metallic, insulating, and semimetallic f-projected densities of states, respectively, at $U = 0$ and within a Fermi liquid phase. We favor intersite V_k due to the similarity of its metallic f DOS to paramagnetic local density results for the rare earths and to the character of their f electrons in the high pressure phases. However, it is to be emphasized that the essential results of this paper are independent of these hybridization choices.

Our calculational approaches are DMFT [2,6,12] and determinant QMC [13,14], carried out for a three-dimensional simple-cubic lattice in the thermodynamic limit and for a 4^3 periodic lattice, respectively. DMFT can capture thermodynamic phase transitions while the quantitative agreement with QMC provides compelling evidence of its accuracy.

Within DMFT, both the f-electron part of the PAM and the HM map onto the same single site problem in which the Green function is calculated from a dynamical mean field $\Sigma_f(\omega)$ [2,6,15]. The difference between PAM and HM is the way ϵ_k^f and V_k enter the self-consistency condition, i.e., the k integrated Dyson equation

$$G_f(\omega) = \frac{1}{(2\pi)^3}\int d^3k\,\frac{1}{\omega - \Sigma(\omega) - \epsilon_k^f - \frac{V_k^2}{\omega-\epsilon_k^d}}\,, \tag{3}$$

where $V_k = 0$ and $\epsilon_k^f = 0$ for the HM and PAM, respectively. In the DMFT equations the d electrons of the PAM, which enter only quadratically, have been integrated out yielding an effective f-electron problem with retarded potential $V_k^2/(\omega - \epsilon_k^d)$. One expects the different potentials to be reflected in quite distinct physical properties of the two models.

The spectral function $A_f(\omega)$ of the f electrons is shown in Fig. 1. At small hybridizations t_{fd}, the PAM spectrum consists of two peaks at $\pm U/2$ which corresponds to a phase with localized f electrons. At larger t_{fd}, an additional Abrikosov-Suhl resonance develops at the Fermi energy which is not gapped for the PAM with intersite hybridization. Thus, the f electrons are itinerant. The striking similarity to the spectral function of the HM (inset) calls for a more quantitative comparison of the crossover between itinerant and localized f electrons which is driven by an increase of $U_f/t_{fd(ff)}$. Such a detailed comparison is the subject of this paper.

In the self-energy Σ_f (Fig. 2a), the crossover [16] shows up as an abrupt change of the behavior with t_{fd}: for large t_{fd} Fermi liquid behavior with $\mathrm{Im}\Sigma_f(i\omega_n) \propto \omega_n$ at low

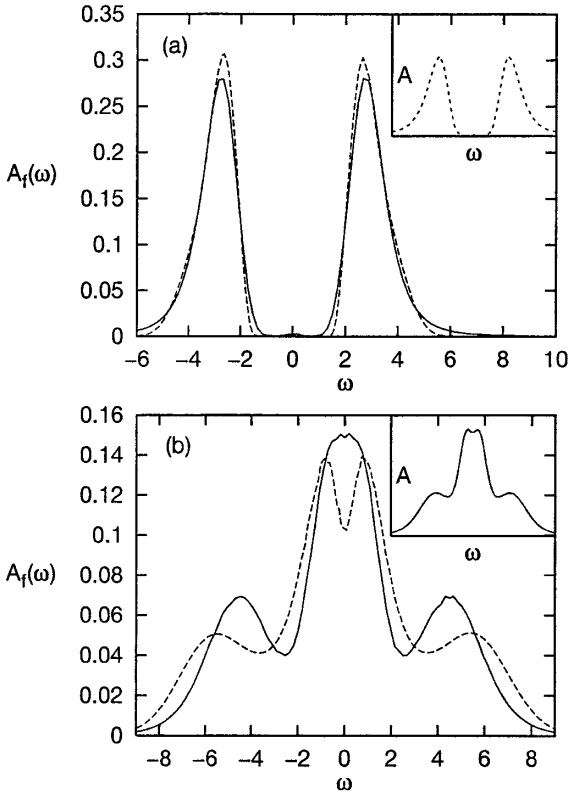

FIG. 1. The spectral function of the PAM at $U_f = 6$ and $T = 0.2$ with an intersite hybridization of (a) $t_{fd} = 0.3$ and (b) $t_{fd} = 1$, respectively, as obtained by DMFT (solid line) and QMC (dashed line). With the exception of a small antiferromagnetic splitting of the central resonance found in finite-d simulations at $t_{fd} = 1$ the agreement between DMFT and QMC is excellent. Insets: HM (DMFT) at $U_f = 6$, $T = 0.2$, $t_{ff} = 0.3$, and $t_{ff} = 1$, respectively.

(Matsubara) frequencies occurs, while at small t_{fd} an insulatinglike behavior with diverging $\mathrm{Im}\Sigma_f$ is observed. From the Σ_f data one can calculate a quantitative measure for the crossover from itinerant to localized f electrons: the quasiparticle weight of the Abrikosov-Suhl resonance $Z_f = [1 - \partial\Sigma_f(\omega)/\partial\omega|_{\omega=0}]^{-1}$ [calculated via finite differential quotient $(1 - \mathrm{Im}\Sigma_f(i\omega_0)/\omega_0)^{-1}$]. Just as at the Mott transition of the HM [1,2,17–19], Z_f vanishes with decreasing t_{fd}/U_f for the PAM. This behavior of the PAM is astonishingly similar to that seen in the HM and is insensitive to the choice of hybridization as is seen in Fig. 2b.

While the important similarity between the two models lies in the presence or absence of the central resonance as a whole (measured by Z_f), the PAM hybridization can determine finer details such as whether this resonance may be split by a gap. Consider the charge compressibility $\kappa_f = \partial n_f/\partial\mu$ shown in Fig. 2c. Nonzero κ_f indicates a metallic phase, while κ_f is exponentially small in $1/T$ within a gapped insulating phase. At small $t_{fd(ff)}$, all f spectral functions show insulating behavior as there are no central resonances lying between the two Hubbard bands. These resonances form in all cases at larger $t_{fd(ff)}$; however, they

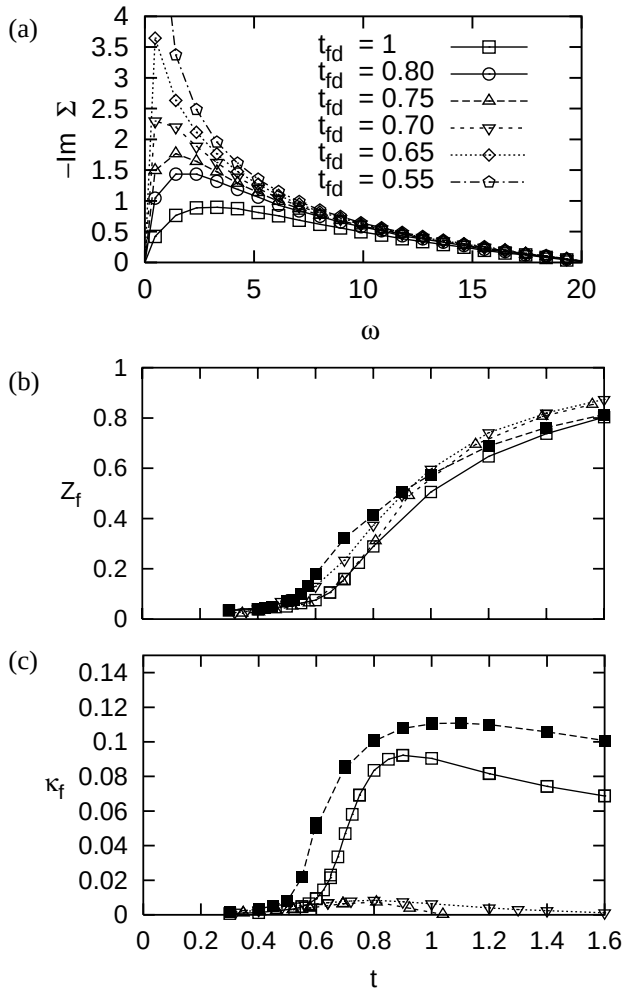

FIG. 2. (a) (Matsubara) frequency dependence of the imaginary part of the self-energy of the PAM with intersite hybridization. The behavior for the HM (not shown) is very similar. (b) Quasiparticle weight Z_f as a function of $t = t_{fd}$ and $t = t_{ff}$ for the PAM and HM, respectively [(□) PAM with intersite, (△) PAM with on-site, and (▽) PAM with odd-parity intersite hybridization; (■) HM]. (c) Electronic compressibility $\kappa_f = \partial n_f/\partial\mu$ as a function of t. All results are calculated by DMFT at $U_f = 6$ and $T = 0.15$ (△, ▽: $T = 0.07$).

are split by insulating and semimetallic hybridization gaps for the on-site and odd-parity cases, respectively, as is evident in Fig. 2c.

While the (unscreened) local moment $\langle m_z^2\rangle = \langle (n_\uparrow - n_\downarrow)^2\rangle$ shown in Fig. 3 decreases with increasing hybridization, it is still quite substantial through the HM and PAM crossovers of Fig. 2, marked by arrows in Fig. 3. This smooth behavior of the local moment from weak to strong coupling in *both* models is insufficiently appreciated in the discussions of the distinctions between the "Mott" and "Kondo" scenarios for the volume collapse transition, where mean-field treatments of the correlations lead to artificially abrupt changes in the local moment. Despite the finite moments, screening effects lead to low-T Pauli (or even gapped) susceptibilities at large $t_{fd(ff)}$.

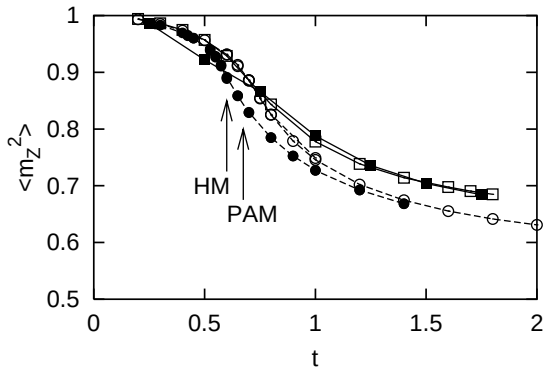

FIG. 3. The square of the local moment is shown as a function of $t = t_{fd}$ and $t = t_{ff}$ for the PAM with intersite hybridization (open symbols) and HM (closed symbols), respectively, at $U_f = 6$ and $T = 0.15$ (circles: DMFT, squares: QMC) ($T = 0.5$ for the QMC HM to avoid antiferromagnetic ordering). In neither case does the moment change remarkably in the vicinity of the transitions of Fig. 2 (arrows).

The T-U_f phase diagrams which result from consideration of the self-energy, quasiparticle weight, and magnetic susceptibility are shown in Fig. 4. Both the HM and PAM have a low temperature phase of antiferromagnetic order with a maximum in the Néel temperature T_N at intermediate U_f/W. At a slightly larger U_f/W, a second transition, i.e., the disappearance of the quasiparticle peak, is observed within the paramagnetic phase (if antiferromagnetism is frustrated). This is the Mott transition of the HM and, from the Kondo point of view, the crossing of the Kondo temperature $T_K(t_{fd})$. Apart from the temperature and hybridization scales, the phase diagrams of HM and PAM are remarkably similar at finite T. It is an open question at present whether such similarities will persist down to zero temperature.

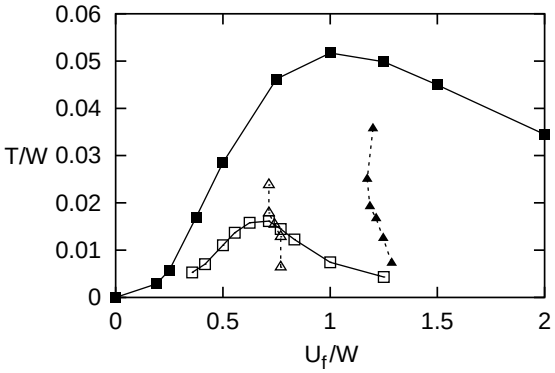

FIG. 4. T-U_f phase diagram of the Hubbard model with a semielliptic DOS (filled symbols; reproduced from [18,20]) and PAM with intersite hybridization (open symbols) within DMFT. Here W is the bandwidth of the Bethe DOS and $12t_{fd}$ for the PAM, respectively. Squares: Néel temperature; triangles: Mott transition/Kondo temperature (the dashed lines end at higher T as the crossover becomes too gradual in U_f/W to allow a precise location).

The present paper has shown a remarkable similarity between the HM and the f-electron system of the PAM which is indeed—after integrating out the d electrons—like a HM with a more complicated retarded potential. Novel numerical results on the spectral functions, charge compressibilities, and local moments show that despite its more complicated potential, the PAM undergoes (at finite temperatures and half-filling) a crossover from itinerant to localized f electrons similar to the Mott transition of the HM. While this similarity is closest for the PAM with intersite hybridization which describes metallic f electrons at large t_{fd}, the vanishing of the central resonance does not depend on the hybridization choice. This crossover and the transition towards antiferromagnetic order yield phase diagrams which have the same topology for both models. Accordingly, the present paper suggests that the physics underlying the Mott [8] (HM) and the Kondo volume collapse scenarios [9] (PAM or its impurity approximation) for the volume collapse transitions in f-electron metals [10,11] may be similar and *not* incompatible. While the Mott transition is continuous at the temperatures considered, the rapid change in the correlation energy, when combined with the smooth contributions from other valence bands, might nevertheless still result in a Maxwell construction giving the thermodynamic instability manifested as the first-order volume collapse in Ce [21].

In regard to local-density calculations, orbitally polarized and self-interaction-corrected applications [22] to the volume-collapse transitions resemble a mean-field solution of the HM, where the transition coincides with a coalescence of the two Hubbard bands and a simultaneous loss of local moment. The implication of the present paper is that regardless of the balance between f-f (HM) and f-valence hybridization (PAM), a *correlated* solution should show some Kondo-like attributes in the collapsed phase, including an analog of the three-peak local DOS, persistence of the local moment, and its screening as deduced from the susceptibility. Local density theory does not show such Kondo-like features in the collapsed phase; however, it does nevertheless yield excellent structural dependence of the total energy [23].

We acknowledge valuable discussions with N. Blümer, P. van Dongen, M. Jarrell, and D. Vollhardt. This work was supported in part by a DOE ASCI grant, the DAAD, the LLNL MRI, the U.S. DOE Contract No. W-7405-Eng-48, and NSF Grants No. DMR9704021 and No. 9985978.

[1] F. Gebhard, *The Mott Metal-Insulator Transition* (Springer-Verlag, Berlin, 1997).
[2] A. Georges *et al.*, Rev. Mod. Phys. **68**, 13 (1996).
[3] J. Hubbard, Proc. R. Soc. London A **281**, 281 (1964).
[4] D. M. Newns and N. Read, Adv. Phys. **36**, 799 (1987).
[5] C. Huscroft *et al.*, Phys. Rev. Lett. **82**, 2342 (1999).
[6] D. Vollhardt, in *Correlated Electron Systems,* edited by V. J. Emery (World Scientific, Singapore, 1993), p. 57; Th. Pruschke *et al.*, Adv. Phys. **44**, 187 (1995).
[7] M. Ulmke *et al.*, Phys. Rev. B **54**, 16 523 (1996).
[8] B. Johansson, Philos. Mag. **30**, 469 (1974); B. Johansson *et al.*, Phys. Rev. Lett. **74**, 2335 (1995).
[9] J. W. Allen and R. M. Martin, Phys. Rev. Lett. **49**, 1106 (1982); J. W. Allen and L. Z. Liu, Phys. Rev. B **46**, 5047 (1992); M. Lavagna *et al.*, Phys. Lett. **90A**, 210 (1982); J. Phys. F **13**, 1007 (1983).
[10] See, e.g., U. Benedict *et al.*, Physica (Amsterdam) **144B**, 14 (1986).
[11] A. K. McMahan *et al.*, J. Comput.-Aided Mater. Design **5**, 131 (1998).
[12] DMFT studies of the on-site hybridization model include the following: M. Jarrell *et al.*, Phys. Rev. Lett. **70**, 1670 (1993); M. Jarrell, Phys. Rev. B **51**, 7429 (1995); A. N. Tahvildar-Zadeh *et al.*, Phys. Rev. B **55**, 3332 (1997); M. J. Rozenberg, Phys. Rev. B **52**, 7369 (1995).
[13] R. Blankenbecler *et al.*, Phys. Rev. D **24**, 2278 (1981).
[14] QMC studies of the on-site hybridization model include the following: J. Bonča and J. E. Gubernatis, Phys. Rev. B **58**, 6992 (1998); Y. Zhang and J. Callaway, Phys. Rev. B **38**, 641 (1988); M. Vekic *et al.*, Phys. Rev. Lett. **74**, 2367 (1995).
[15] The DMFT single site problem is solved numerically following J. E. Hirsch and R. M. Fye, Phys. Rev. Lett. **56**, 2521 (1986).
[16] While the transition observed is not first order (at the temperatures considered), it is very difficult to decide numerically whether it is a second-order phase transition or noncritical. We use the word "crossover" to express our expectation that it is noncritical without excluding the possibility that it is second order.
[17] W. F. Brinkman and T. M. Rice, Phys. Rev. B **2**, 4302 (1970).
[18] J. Schlipf *et al.*, Phys. Rev. Lett. **82**, 4890 (1999).
[19] R. M. Noack and F. Gebhard, Phys. Rev. Lett. **82**, 1915 (1999); R. Bulla, Phys. Rev. Lett. **83**, 136 (1999).
[20] N. Bulut *et al.*, Phys. Rev. Lett. **72**, 705 (1994); M. Ulmke *et al.*, Phys. Rev. B **51**, 10 411 (1995).
[21] We obtain energy difference curves for the present DMFT PAM results quite similar to the QMC results in Fig. 2(a) of [5], with slope changes near $t_{fd} \sim 0.6$ of $\partial \Delta F / \partial \ln t_{fd} \sim 0.4$ eV for *both* on-site and even-parity nearest-neighbor hybridizations (the only two tested), which as noted in that paper are in order of magnitude agreement with experiment.
[22] O. Eriksson *et al.*, Phys. Rev. B **41**, 7311 (1990); A. Svane *et al.*, Phys. Rev. B **56**, 7143 (1997); Z. Szotek *et al.*, Phys. Rev. Lett. **72**, 1244 (1994); A. Svane, Phys. Rev. Lett. **72**, 1248 (1994); Phys. Rev. B **53**, 4275 (1996).
[23] P. Söderlind, Adv. Phys. **47**, 959 (1998).